Reconfigurable Patterns of Photovoltaic Cells to Reduce Power Loss due to Detrimental Shading Conditions

Alexander Eick[1], João Paulo Hanke de Faria[1], and Davies William de Lima Monteiro[1,2]

[1]Laboratory for Optronics and Microtechnology Applications, UFMG, Belo Horizonte, MG, 31270-010, Brazil
[2] Department of Electrical Engineering, UFMG, Belo Horizonte, MG, 31270-010, Brazil
e-mail: alexander.eick@outlook.com

***Abstract*— Poorly illuminated or defective photovoltaic cells (PV cells) affect the performance of the whole panel. In this work, we propose a methodology to discover the best connection pattern among cells in a panel under unfavorable shading conditions. It is, therefore, assumed that the target PV module allows internal disconnection and reconnection of neighboring cells. In order to manage the reconfiguration of the cells on the array, the developed algorithm searches for the connection pattern that yields the least power loss, taking into account the cell model in silicon and the effect of shading. Three progressive shading schemes have been applied to mimic possible hard shading on a 36-cell panel. For each case, the algorithm analyzed the IV-characteristics of the panel and suggested the best cell-connection pattern to achieve the highest power output under each condition. When less than 15 of the 36 PV cells were affected by shading, the algorithm was able to present up to 30% reduction in power loss when compared to the standard configuration, and up to 20% reduction when compared to complex fixed connection patterns. For shading patterns where 15 or more PV cells were affected, reconnection of the cells did not result in a reduction of power loss. However, if the PV panel is properly installed, only marginal hard shading should be expected and the algorithm would represent a promising tool. It could be deployed dynamically by means of switches and a management unit coupled to the panel. The reconfiguration methodology herein proposed can as well be utilized for photovoltaic energy harvesting in integrated autonomous microsystems.**

***Index Terms*— photovoltaic array; reconfigurable photovoltaics; smart photovoltaics; algorithm; BIPV**

I. Introduction

The most often detrimental condition to a photovoltaic solar panel or plant is shading. It is usually partial, which means either partial but uniform light intensity, partial spatial blockage of light, or both. This can be caused by clouds, which provide more fluent shading edges and more variation in shading level within the shaded area; by dust, leaves and other accumulated clutter; by nearby moving objects, as tree branches; or by hard structures, like houses, billboards, poles, etc. These latter objects provide well defined shading borders as well as even shade distribution, which will be called hard shading and used in this work. Examples of hard shading can be found in PV panels installed on rooftops in urban areas, where adjacent buildings might provide partial shading during some time of the day, and in urban power plants, which are located in sub-optimal locations. An example is the plant on the roof of Mineirão soccer stadium in Belo Horizonte, Brazil [1], where the PV panels are regularly affected by shading from the buildings architectural indentations, leading to regular energy loss.

As partial spatial shading affects the performance of a whole panel, sometimes as much as if the array was totally shaded, a reconfigurable photovoltaic array could be useful. In it the connection pattern could be changed, minimizing the deleterious influence of the shaded cells. The idea of a reconfigurable photovoltaic array, a string of multiple PV panels, was first patented in 1979 by Gruber [2]. The author describes photovoltaic panels in which some of the cells can be reconfigured to achieve different series-parallel connections to transfer the maximum power to the connected load. In 1990 Salameh and Dagher proposed to improve the performance of stand-alone water pumps powered by photovoltaics using reconfigurable solar panels [3]. In 1998 Auttawaitkul et al. proposed a method to improve the acceleration of PV powered cars, using PV array reconfiguration [4]. In the 21^{st} century already multiple patents were filed [5, 6] and various research groups proposed methods and mathematical models to reconfigure photovoltaic arrays depending on the partial shading conditions [7, 8, 9, 10].

The aforementioned papers can be divided into two groups. The first group assumes that the array is fully reconfigurable [3, 4, 6, 8, 9], i.e. all panels/cells can be connected to all other panels/cells. The second group, on the other hand, assumes that the array is only partially reconfigurable [5, 7], i.e. the PV array consists of a fixed part and an adaptive part, which can be connected to every string of the fixed part. In this second group, there was also work on groups of cells in a panel monitored and connected to smart DC-DC converters to improve the contribution of the respective shaded cluster [11, 12].

In 2002 a patent was granted to Sherif and Boutros which describes in very general terms a reconfigurable photovoltaic panel very similar to the one proposed in this work, meant for spacecraft applications [6]. Their work, however, fails to provide any specific proposal for a reconnection algorithm, based on different shading conditions, that could support the actual feasibility of such a system.

Despite different approached, both groups assume a reconfigurable connection between PV panels. Furthermore, they generally use one reference cell to determine the environmental conditions for multiple PV cells connected to the panel or even complete PV panels. In this scenario, the mathematical models might provide erroneous predictions or fail altogether, if a solar panel suffers from partial shading and its I-V characteristics are significantly deteriorated. Due to the

Digital Object Identifier 10.29292/jics.v15i3.134

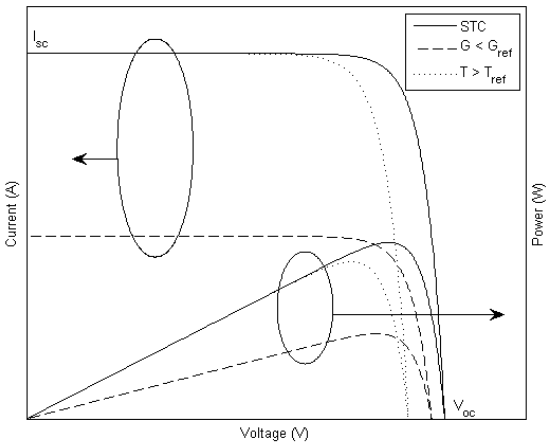

Fig. 1 I-V and P-V characteristics of a typical photovoltaic panel under the influence of different irradiance and temperature values.

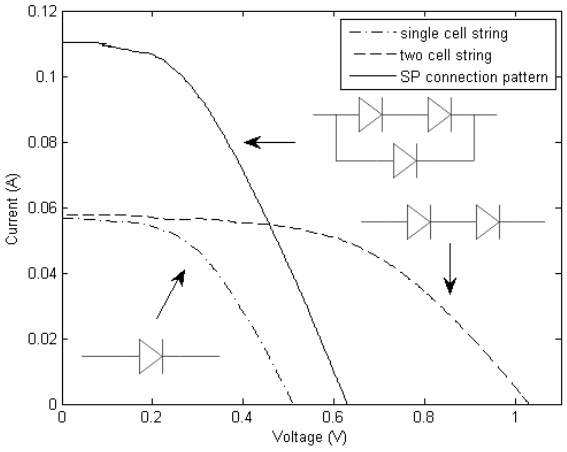

Fig. 2 I-V characteristics of: a separate PV cell, a series connection of two cells in a string, and connection of a two-cell series string in parallel to a single cell. [13, Figure 13]

fact that the condition of the reference cell may not reflect the condition of the other panels.

In this work, however, a reconfigurable connection between the photovoltaic cells is assumed. In addition, each one of these cells could be monitored to extract information about its operating condition, e.g. irradiance and temperature. This information could be used to determine if a particular PV cell is shaded or affected by any other detrimental effect, as debris, hot spots, optical and mechanical defects. Therefore, each individual cell would provide accurate data of the PV panel condition and, thus, the proposed algorithm could find the optimal connection pattern to maximize the power output, even though parts of the panel are shaded.

The partial shading in this work is assumed to be hard shading. The algorithm can be adapted to predict patterns for both panels and panel strings in power plants, or even those of PV cells in a microsystem. They could be deployed to either charge an energy-storage component or to directly supply the necessary voltage to integrated circuits and sensors. Our proposal uniquely provides a detailed and practical description of such a reconfigurable PV panel and a methodology to find the reconfiguration of choice, together with an analysis of the possible power gains in it. Hereby it is assumed that each cell can only be connected to its immediate neighbors in a predefined grid, limiting the amount of switches and additional wiring needed.

Shading is one of the factors that influences the typical ideal characteristic curves (current and power) of a photovoltaic panel for a given reference irradiance (G_{ref}) and temperature (T_{ref}), as shown in Fig. 1. Furthermore, the effects on the panel response due to lower irradiance and higher temperature are shown. Internal parameters of the cells composing the panel, interconnections and encapsulation might effect a change to the ideal curve as well, but these will not be considered in the scope of this work.

After extensive research on already existing connection patterns (section II) and on the materials and methods used in this work (section III), we developed an algorithm (section IV) to manage reconfigurable connections between PV cells to adapt them to different shading conditions. Our simulation results are presented in section V and discussed in section VI. Lastly, in section VII, we present our conclusions.

II. Connection patterns

Different cell arrays and connection patterns attend to a variety of load current and voltage requirements. The simplest connection patterns used are the series and the parallel associations, meant to scale the overall voltage or current output, respectively. Oftentimes, a mixed series-parallel (SP) association is used, which scale both the voltage and the current.

While connecting multiple solar cells in a panel, it is important to use cells with identical or nearly identical electrical characteristics to avoid that the performance is dominated by the least efficient ones. Thus altering the expected I-V characteristics. In a series connection, for instance, the current through the branch is limited by the cell that generates the lowest current. Therefore, even if the cells are identical, partial shading of one cell limits the current of the series association.

To visualize the effects of mismatch losses in terms of asymmetrical number of cells in parallel strings, Eick performed some simple experiments to show the impact on a SP connection pattern [13]. Fig. 2 shows the results obtained for the V_{oc} mismatch losses when a cell is missing on one of the parallel strings, for instance, due to a short circuit. In chapter 2.3.5 of that work, the author characterizes the behavior of a V_{oc} mismatch (shown in Fig. 2) and concludes that it works similar to the more well known I_{sc} mismatch, i.e. the resulting V_{oc} of the association is dominated by the lowest V_{oc} present on the parallel strings.

Thus, when single cells in a series (S), parallel (P) or series-parallel (SP) connection are affected, the output of the whole array is deteriorated. The most common and ubiquitous solution to avoid the shaded element is the use of a bypass diode in parallel to the element. They are more commonly employed for whole panels in an installation, than for individual cells. The bypass diode, however, alters the I-V curve and can introduce multiple local maximum-power points, masquerading the global maximum-power

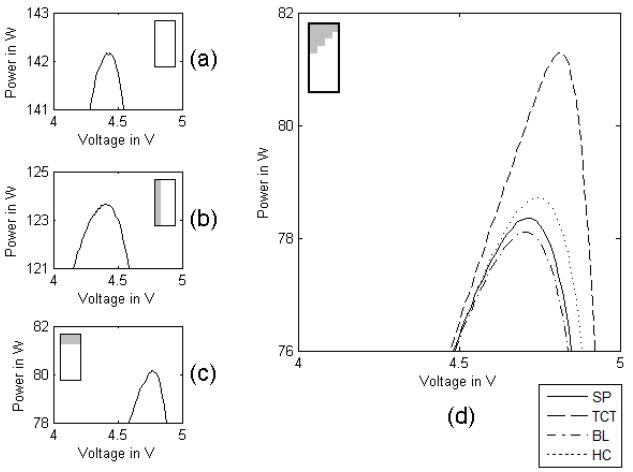

Fig. 3 P-V characteristics of different connection patterns of a 9x4 cell photovoltaic panel under varying shading, i.e. no shade (a), vertical shade (b) horizontal shade (c) and diagonal shade (d). [13, Figure 15 & 16]

point when Maximum-Power-Point Trackers (MPPT) algorithms are used [14]. Smart bypass solutions for panels and panel strings have also been proposed based on semiconductor monolithic switches with and without a control unit to reduce the power loss compared to the bypass diode [15, 16, 17]. Neither the bypass diode, nor these smart bypass solutions prevent hot-spot heating, nor have been combined with a reconnection strategy for the illuminated cells.

Other recently proposed options [18, 19, 20], focus on an increased number of fixed internal connection configurations. Namely, the total cross-tied (TCT), the bridge-linked (BL) and the honey-comb (HC) configurations [20, Figure 1(d-f)]. They present additional parallel connections to introduce multiple redundancies that equal the voltage and current over the panel. Through these additional ties, the panels are able to mitigate the deterioration of the output due to practically unavoidable mismatch losses between cells. Thus improving their performance under partial shading. Their performance has been evaluated by various researchers and found to be superior to S and SP connections under various shading conditions [16, 17, 13].

The differences in performance between the various connection patterns is shown in Fig. 3. It can be seen that there is virtually no difference between the P-V characteristics and the curves overlap for the first three conditions (Fig. 3(a), (b), (c)). Only for the last condition (Fig. 3(d)), when shading is diagonally extended over the panel, a difference in performance can be seen. Most of the complex connection patterns perform better than the SP connection pattern in the diagonal shading. When compared among each other, the TCT configuration is able to extract the most power from the panel, due to the larger number of ties it features. [20].

When vertical or horizontal shading is present, however, the complex connection patterns are not able to noticeably improve the performance compared to the standard SP configuration. Especially under those circumstances, other techniques have to be devised, e.g. reconfigurable arrays. In this article we will show that a reconfigurable SP array can theoretically yield better power performance for moderate shading expanding vertically and for moderate diagonal shading. For moderate shading expanding horizontally, the performance is kept at approximately the same level as that of the complex configurations. The highest gain is observed for diagonal shading.

III. Materials & Methods

There are many technologies and materials to fabricate photovoltaic cells, and the methodology herein proposed is technology agnostic, provided that the I-V characteristics are known. However, nowadays, the majority of commercially available PV panels is assembled using silicon cells. The panel used as a basis for our simulations is assembled with poly-crystalline silicon solar cells (Kyocera KD140SX-UFBS). Its 36 cells are connected in series to achieve a rated peak power output of 140 W. The following nominal electrical parameters are used to determine the electrical parameters of each cell to be set in the simulation: $I_{sc} = 8.68\ A$, $V_{oc} = 22.1\ V$, $I_m = 7.91\ A$, $V_m = 17.7\ V$, $\beta_{I_{sc}} = 0.060\ \%/°C$, $\beta_{V_{oc}} = -0.36\ \%/°C$, $NOCT = 45\ °C$. $\beta_{I_{sc}}$ and $\beta_{V_{oc}}$ are the temperature coefficients at the short-circuit current and the open-circuit voltage, respectively.

A. Shading

Shading can come in many shapes and can be caused by a variety of objects, but it can generally be divided in distinctive groups. First of all, shade can be classified as dynamic or static. Here, dynamic describes a shade that moves over the panel rapidly and unpredictably, e.g. clouds which provide unpredictable shading during the day. Static shading, on the other hand, is provided by immobile objects, e.g. buildings. Both shading groups reduce the panel efficiency. However, the effects of static shade can be better predicted while planning and installing the photovoltaic panel, although they are perhaps unaviodable.

Shading can still be divided into two other categories, i.e. complete and partial cell shading. If any object is overcasting only parts of a given PV cell, then the power output of this particular cell is reduced. However, it is not as low as if the PV cell is completely shaded, which would generate a significantly lower output power, or none. If the shading is hard and complete it is also know as hard shading, when no light whatsoever reaches the shaded regions of the cell.

For the scope of this work, it has been assumed that any shaded PV cells in an array is completely hard shaded. The developed algorithm is able to deal with dynamic shading as it can be employed to reevaluate the situation periodically. In case of a predictable shading pattern throughout the year, it is possible to run the algorithm only once and program each preset reconfiguration pattern to be deployed at specific seasons.

B. Physical switches, circuits and integration

Even though the physical composition of the reconfigurable panel depends on each particular installation, purpose and technology used, an example of preliminary ideas of its electrical connection can be seen in Fig. 4. It is inspired by [6] in a 4x4 panel, where every cell is connected to its neighbors by switches. Here, switches can be of different kinds and designs, but transistors might be the best choice, since

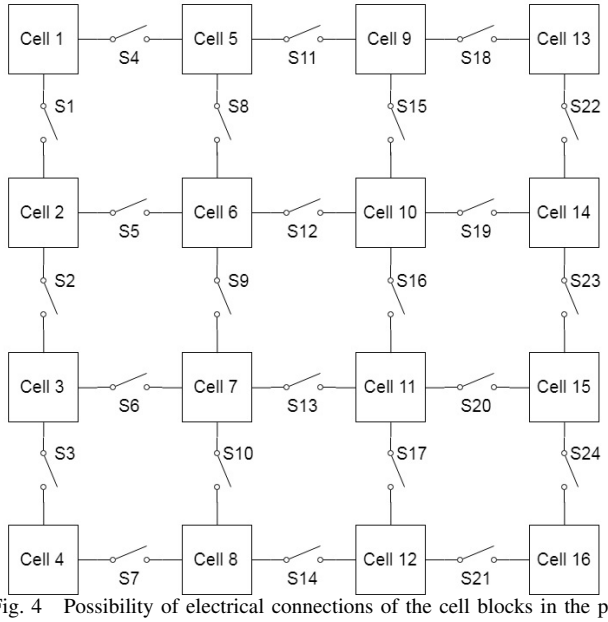

Fig. 4 Possibility of electrical connections of the cell blocks in the proposed PV panel.

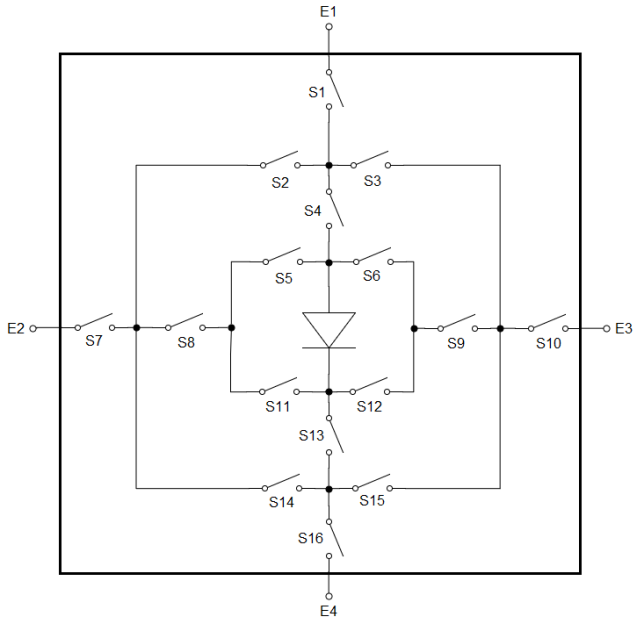

Fig. 5 Electrical schematic of a cell block in the proposed PV panel design.

they require no moving parts and could even be embedded in the panel during assemblage.

The cells, seen in Fig. 4, are cell blocks that include the photovoltaic cell as well as 16 switches to ensure that sufficient alternative connections can be achieved. A schematic for such a cell block can be seen in Fig. 5. In the center, the photovoltaic cell is represented as a diode and around it there are two concentric connection rings equipped with switches along and between them.

The two internal ring interconnects ensure that the cell block is always able to connect the PV cell regardless of which of the four external connections is connected to the anode or to the cathode of the diode. For example, when the external connection E1 is meant to be the anode and E4 the cathode, all switches are open, except S1, S4, S13 and S16, which are closed to allow the current to flow. However, if E4 is meant to be the anode and E3 the cathode, then switches S16, S14, S2, S4 are closed to enable the connection from port E4 to the anode of the PV cell. To connect the cathode to port E3, switches S12, S9 and S10 have to be closed. Besides them, all other switches need to be open. This ensures that the cell blocks can be included in every connection pattern deemed to be the best suitable under a specific shading condition.

The panel, however, still needs control circuits, which could be created on lower layers, as in employing a micro controller, switch drivers and a processor to run the algorithm. Lower layers could as well be an option to connect the ends of a cell string to the positive and negative connection terminals of the panel. The cell status could be monitored by sensors integrated to the system. Each cell can act as its own sensor, considering that the pn-junction characteristics are dependent on the temperature and on the amount of light impinging on it.

A central monitoring unit could probe each cell by momentarily activating bypass current drains. For this monitoring, it is possible to use a microcontroller that stays in low-power mode for most of the time and, from time to time, wakes up, measures the conditions of the PV panel, and manages the reorganization of the cells. To reduce, even more, the power and run time spent in the process, a ”calibration” could be provided in a way that the best configuration for each possibility of shadowing would be stored in the memory of the microcontroller beforehand. This way, when the microcontroller is probing the cells, and determining which will be disconnected, the switches will be instantly activated to achieve the desired configuration.

The advantages of this approach are: the possibility to find commercial microcontrollers with very low power consumption (especially in stand-by or sleep modes) at very reasonable costs, and the program to control this will not be very complex, as it is basically a look-up table. The challenges, however, are in the amount of switches used in this proposition. As observed in Fig. 5, each PV cell requires 16 switches to be able to reconnect with any of its neighbors, not to mention the switches between the cells (Fig. 4). Dealing with this amount of switches might demand a microprocessor with a large memory size to store and control the states of all switches.

To tackle this issue, there is the option to design an additional circuitry with very low power consumption to hold the state of the switches when the MCU is on stand-by/sleep mode. Another alternative is to use MCUs already available on the market in a master/slave setup: a master, to identify the state of the switches and pass them to the other controllers, and the slaves, responsible only for holding the states of the switches, without the need of any kind of oscillator, ADC/DAC or another system with high power consumption.

In regular PV panels, as the commercial one used for the simulations, the switches used between the cells must be designed to handle currents on the order tens of amperes, as the current can become very high as the number of PV cells or strings in parallel increase. This demand on handling mod-

erate to high currents depends on the photocurrent generation capacity of each cell, on the maximum number of cells that can be connected in parallel, and may exceed hundreds of amperes. Current manufacturing process of photovoltaic cells would be already more compliant with the integration of transistors as they often deploy lower dopant concentration than in microelectronic processes. Therefore being more suitable for power switches. If the array is integrated on a chip, on the other hand, very small maximum currents are expected.

C. Electrical Model

To evaluate photovoltaic applications, the I-V characteristics of the separate PV cells and those of the whole panel have to be simulated. For this purpose, various analytical models have been proposed in the literature such as the one-diode model and the two-diode model [21], where intrinsic semicondutor physical and constructive parameters are used alongside the interaction between light and the material.

However, the model used in this work is the electrical behavioral model in PSPICE, using a combination of controllable current and voltage sources together with diodes and resistors [22]. In it, only electrical parameters, provided by the PV cell manufacturer at STC are used to simulate the photovoltaic cell. The necessary parameters are the open-circuit voltage (V_{oc}); the short-circuit current (I_{sc}); voltage and current at the maximum-power point (V_m and I_m); temperature coefficient of the open-circuit voltage and of the short-circuit current; and the nominal operating cell temperature (NOCT). Parameters can then be estimated for a given irradiance and a given temperature. Intrinsic parameters, as the pn-junction dark reverse saturation current and series resistance, can also be calculated. The series resistance is usually calculated at reference condition and was assumed to be independent of temperature and irradiance in [22]. However, Eick showed that this is not the case and adapted the original model to account for the influence of these factors on the series resistance [23].

IV. The Algorithm

To simulate the effects of the reconnection of photovoltaic cells within the panel on the overall panel output, a MATLAB algorithm was written. It takes into account the cell behavior model with irradiance and temperature as environmental parameters. Fig. 6 shows the flowchart of this algorithm, with the first four steps as described.

The algorithm then uses various subroutines to:

- Find coequal partitions;
- Generate I-V curves for all possible configurations when all cells are interconnected;
- Generate I-V curves for all possible configurations when only fully illuminated cells are interconnected;
- Analyze all I-V curves and find configurations within the chosen margin around the maximum-power point;
- Find a possible cell reconnection pattern.

In number theory "a partition of a number n is a representation of n as the sum of any number of positive integral parts." [24]. However, in the context of this work only a subset of those partitions is of interest, i.e. only the partitions that consist of the same positive integers. Those partitions are therefore coined as "coequal partitions". The reason for that lies in the fact that only strings with an equal number of cells in series N_s are to be connected in N_p parallel strings. Otherwise there is always a reduction in the V_{oc} of the composition, limited by the string with the lowest V_{oc}, i.e. the one with less cells in series. If an arbitrary panel has 16 illuminated cells, they can be interconnected as expressed by the 5 possible coequal partitions:

$$\{1+1+1+1+1+1+1+1+1+1+1+1+1+1+1+1\}$$
$$(N_s = 1,\, N_p = 16),$$
$$\{2+2+2+2+2+2+2+2\}$$
$$(N_s = 2,\, N_p = 8),$$
$$\{4+4+4+4\}$$
$$(N_s = 4,\, N_p = 4),$$
$$\{8+8\}$$
$$(N_s = 8,\, N_p = 1),$$
$$\{16\}$$
$$(N_s = 16,\, N_p = 1).$$

Table I shows the results for each of these reconnection patterns for cells with nominal parameters given in the same table.

The algorithm needs to be able to model a panel from the behavioral characteristics of its composing PV cells in different reference configurations (series, parallel and mixed series-parallel). It needs to model local changes in irradiance and temperature throughout a panel, and it needs to automatically find the most suitable reconnection pattern among cells under a certain shading condition. In order to be more realistic in terms of physical interconnect bus implementation, we have restricted the reconnection possibilities of any cell in the array to only those cells in its immediate neighborhood. When cells are shaded, they may be disconnected and the algorithm will search the coequal partition, considering the effective number of illuminated cells, that yields the highest power closest to the maximum-power point of the original configuration within some pre-defined voltage boundaries. In some situations, however, keeping the shaded cells connected offers a better result. If cells 1, 5, 6 and 9 in the previously evaluated 16-cell panel are shaded, the algorithm finds the best reconnection pattern to be that shown in Fig. 7. Here the shaded cells are disconnected and the 12 remaining ones are connected in 4 parallel strings, each with 3 cells ($N_s = 3$, $N_p = 4$).

In its current version, the algorithm can determine and analyze the best configuration pattern for any shaded SP photovolatic panel when the electrical characteristics are know. Only the panel size and its electrical characteristics have to be initially set. Even non-silicon PV panels can be modelled provided an suitable electrical model, to determine their I-V characteristics, is available. However, there is still plenty of room for improvement, especially for the search engine

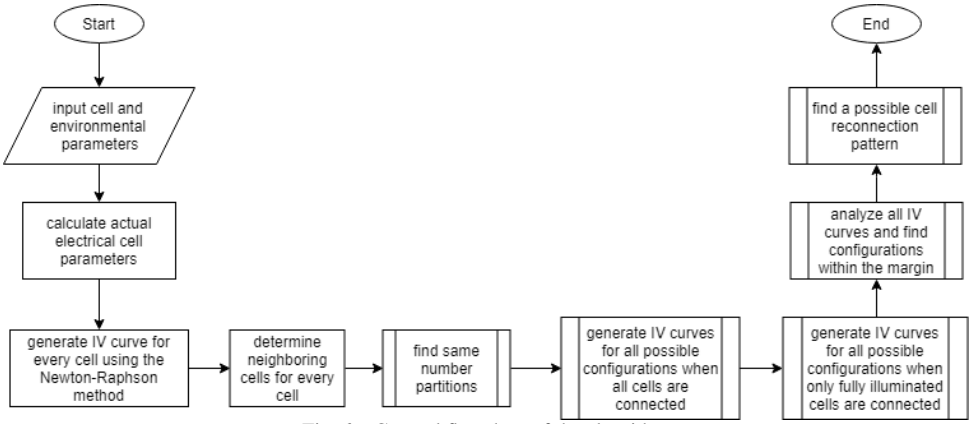

Fig. 6 General flowchart of the algorithm

Table I Simulation of the key parameters for different connection patterns (coequal partitions) for 16 cells.

Parameters	Connection Pattern					
	Single cell	$N_s = 16$ $N_p = 1$	$N_s = 8$ $N_p = 2$	$N_s = 4$ $N_p = 4$	$N_s = 2$ $N_p = 8$	$N_s = 1$ $N_p = 16$
$I_{sc}(A)$	8.68	8.68	17.39	34.72	69.44	138.88
$V_{oc}(V)$	0.61	9.82	4.91	2.46	1.23	0.61
$P_m(W)$	3.89	62.21	62.21	62.21	62.21	62.21
$I_m(A)$	8.17	8.17	16.34	32.67	65.34	130.69
$V_m(V)$	0.48	7.62	3.81	1.90	0.95	0.48

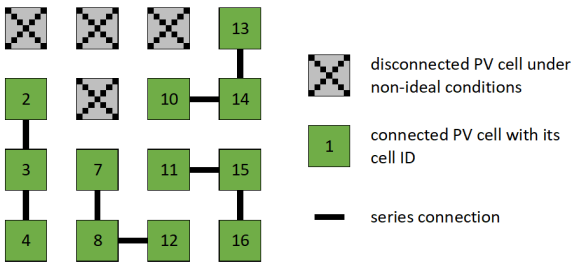

Fig. 7 Result for the reconnection of the test panel.

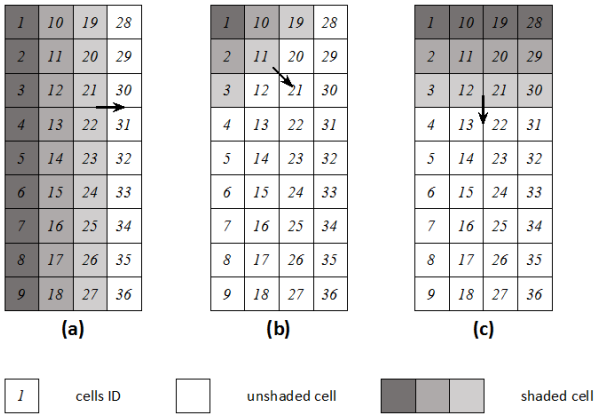

Fig. 8 Progressive shading patterns of the simulated PV panel.

of the reconnection sub-algorithm. As it has been implemented, this part finds the best reconnection pattern by extensive sequential searching. Therefore, depending on the shading pattern and the computing power it can take very long to find a solution. Especially when the algorithm fails to achieve the best suitable connection pattern, and thus, the second best pattern has to be used instead. When this happens, the algorithm can take days to find the solution. For this reason, applying it in real time is not yet an option. However, depending on the application, it can be used to set a static connection pattern, thus being executed a single time during the setup of the application. Another possible application could be to predetermine various connection patterns, through which the panel can switch dynamically according to preset factors, e.g. time of the day or time of the year.

A more detailed explanation of the algorithm can be found in [13]. In it the various subroutines are explained in detail as well.

V. Results

In this work, only shading by clear geometrical shapes, such as that caused by houses, walls or billboards, is considered. Those shading patterns often start at the sides or corners of a panel. Therefore three different general approaches are analyzed. Firstly, the shade is swiping in from the left, covering the panel column by column (see Fig. 8(a)). Secondly, a shade diagonally swipes in starting in the left upper corner as seen in Fig. 8(b). And thirdly the shade swipes in from the top, covering the panel row by row (Fig. 8(c)). Here, the gray tones in Fig. 8 symbolize the displacement of the shade and each cell is considered to be shaded completely. Thus, when the shade swipes in from the left, only the first column is shaded completely in the beginning. Subsequent simulations will deal with the first two columns, the first three and at last all columns being shaded.

Considering a model panel, based on the Kyocera KD140SX-UFBS PV module (section III.), subjected to an irradiance $G = 500\ W/m^2$, we performed 26 simulations representing different levels of shading. These results are shown in table II. The connection pattern chosen as a standard reference was that with the 36 cells connected with $N_s = 12$, $N_p = 3$, i.e. 3 strings of 12 cells, hereby referred to as the SP standard connection. The voltage boundaries were arbitrarily set at $\pm 20\%$ of maximum-power point voltage of $V_m = 5\ V$ of the reference configuration at $G = 500\ W/m^2$, and the lowest maximum-power boundary at -20% of the maximum power of the standard configuration $P_m = 122.81\ W$. There are 104 coequal partitions, of which only some will yield V_m and P_m compliant to the established boundaries, and the best of them will be shown for each simulation. The row for each simulation corresponds to the best connection pattern found by the algorithm. In some cases, the standard configuration is the only possible pattern, as will be explained below. The number of cells N_c may vary, as a configuration disconnecting some cells might yield better results than those with all cells connected. Even when the standard reference pattern does not stand in the two best ranked results, its results are shown in the table for comparison, as is the case for simulation 8. Table II also presents the power loss Δ_P compared to that of the standard connection configuration under full illumination.

Simulation 1 considers the PV panel under ideal conditions and shows its two best connection patterns. Simulations 2 - 5 refer to Fig. 8(a) and describe the shade sliding in from left to right. Simulations 6 - 17 describe diagonal shading starting from the top left corner, as shown in Fig. 8(b). And simulations 18 - 26 are referring to Fig. 8(c) and describe a horizontal shading pattern starting from the top.

In general, it was found that all suitable configurations need to have at least 10 photovoltaic cells connected in series to provide a voltage at the maximum power point of at least $4V$, the lower voltage limit, and a maximum of 14 cells connected in series, not to exceed the upper voltage limit of $6V$. Depending on the number of available illuminated cells, multiple strings can be connected in parallel to achieve higher currents and consequently higher power outputs. However, all simulations where more than 26 PV cells are shaded yield the standard configuration as the only suitable pattern, since no other configuration can provide the required voltage at the maximum-power point. In all cases a series-parallel (SP) connection was found as optimal by the algorithm.

Summarizing the above presented results, it can be seen that reconnecting the photovoltaic cells within a PV panel can decrease the power loss significantly. However, that depends largely on the number of shaded cells and the shading pattern.

In the first set of shaded simulations, simulations 2 - 5, reconnection of the panel does not decrease the power losses. The shade is moving in from the left to right and covers complete columns of the PV cells. Due to the connection pattern of the standard configuration, the parallel strings are not all affected immediately. For example, in simulation 2 only one parallel string of the standard configuration is affected and in simulation 3 only two are affected. And thus the power reduction for the shaded standard configuration is less prominent. Therefore, disconnecting shaded cells and reconnecting the non-shaded cells will not result in power loss reduction.

For the second set of simulations, simulations 6 - 17, the algorithm is able to achieve significant power loss reductions for simulations in which a maximum of 16 PV cells are shaded. This limit means that two parallel strings with at least ten solar cells each can be formed, considering a minimum of 20 non-shaded cells. This would result in a slightly higher power than the shaded standard configuration and subsequently in a lower power loss. Therefore, power loss reductions between 7.5% and 20.5% can be achieved for simulations 6 - 10. For the other simulations in this set (11 - 17) no reduction in power loss can be found when reconnecting the illuminated cells.

In the last set of simulations, i.e. simulations 18 - 26, it was possible to achieve power loss reductions for the first four simulations. These reductions range between 4% and 32%, depending on the shading pattern. In this set, the shade is moving top-down, covering the PV panel row by row. Therefore, since in simulation 18 all four parallel strings of the standard configuration are affected, the maximum power being generated is reduced significantly. Once the number of illuminated solar cells drops below 20, in simulation 22 onwards, the algorithm cannot reconnect the cells in a pattern which would reduce the power loss.

As a last step, the results obtained for the best suitable configuration output by the algorithm, for each shading condition, are compared to simulation results of PV panels using the fixed complex internal connection patterns introduced in section II. Due to the unavailability of datasheet parameters for the TCT, BL and HC patterns, the electrical behavioral model could not be applied to them for MATLAB simulations. Therefore, we employed SPICE using the two-diode model([21]), for which the IV-characteristic and the physical parameters of one photovoltaic cell, I_{01}, I_{02}, n_1, n_2, R_s and R_p, were determined using the software 2/3-Diode Fit developed by [25] for all connection patterns. It includes the SP configurations output by the algorithm.

The results for these comparisons can be seen in table III, which shows the key parameters for each configuration for the four specific connections. There are minor differences in the results of the SP connections in this table, compared to table II, because these values were found with SPICE simulations instead of MATLAB. Therefore, the only meaningful comparisons that can be made are among results presented in this table.

VI. Discussion

Table III shows the results of the comparison of four configurations, i.e. SP, TCT, BL and HC. However, this table only shows the simulations in which an improved reconnection pattern for the SP configuration could be found compared to the standard SP configuration ($N_s = 12$, $N_p = 3$). Therefore, simulations 4 & 5, simulations 11 - 17 and 22 - 26 have been omitted. The exception is simulation 1, in which there is no shading. The power loss Δ_P in this table relates

Table II Maximum power and power losses for optimal connection configurations under different shading conditions.

		N_c	N_s	N_p	P_m (W)	Δ_P (W)	Δ_P (%)
simulation 1		36	12	3	122.81	0.00	0.00
		33	11	3	112.57	10.24	8.34
simulation 2		36	12	3	102.79	19.59	15.95
		26	13	2	88.69	34.12	27.78
simulation 3		36	12	3	82.83	39.98	32.55
		14	14	1	47.76	75.05	61.11
simulation 4		36	12	3	63.03	59.78	48.68
simulation 5		36	12	3	63.03	59.78	48.68
simulation 6		33	11	3	112.57	10.24	8.34
		36	12	3	102.79	19.59	15.95
simulation 7		33	11	3	112.57	10.24	8.34
		36	12	3	102.79	19.59	15.95
simulation 8		30	10	3	102.34	20.47	16.67
		28	14	2	95.52	27.29	22.22
		36	12	3	82.83	39.98	32.55
simulation 9		26	13	2	88.69	34.12	27.78
		36	12	3	63.03	59.78	48.68
simulation 10		22	11	2	75.05	47.76	38.89
		36	12	3	63.03	59.78	48.68
simulation 11		36	12	3	63.03	59.78	48.68
		14	14	1	47.76	75.05	61.11
simulation 12		36	12	3	63.03	59.78	48.68
		14	14	1	47.76	75.05	61.11
simulation 13		36	12	3	63.03	59.78	48.68
		10	10	1	34.11	88.70	72.23
simulation 14		36	12	3	63.03	59.78	48.68
simulation 15		36	12	3	63.03	59.78	48.68
simulation 16		36	12	3	63.03	59.78	48.68
simulation 17		36	12	3	63.03	59.78	48.68
simulation 18		30	10	3	102.34	20.47	16.67
		36	12	3	63.03	59.78	48.68
simulation 19		28	14	2	95.52	27.29	22.22
		36	12	3	63.03	59.78	48.68
simulation 20		24	12	2	81.87	40.94	33.34
		36	12	3	63.03	59.78	48.68
simulation 21		20	10	2	68.23	54.58	44.44
		36	12	3	63.03	59.78	48.68
simulation 22		36	12	3	63.03	59.78	48.68
		14	14	1	47.76	75.05	61.11
simulation 23		36	12	3	63.03	59.78	48.68
		12	12	1	40.94	81.87	66.66
simulation 24		36	12	3	63.03	59.78	48.68
simulation 25		36	12	3	63.03	59.78	48.68
simulation 26		36	12	3	63.03	59.78	48.68

Table III Key parameters for the best SP connection pattern and the three complex fixed connection patterns (TCT, BL and HC).

		I_{sc} (A)	V_{oc} (V)	P_m (W)	Δ_P (%)	I_m (A)	V_m (V)
simulation 1	SP	26.53	6.64	125.14	0.00	24.63	5.08
	TCT	35.37	4.98	125.14	0.00	32.84	3.81
	BL	35.37	4.98	125.14	0.00	32.84	3.81
	HC	35.37	4.98	125.14	0.00	32.84	3.81
simulation 2	SP	22.11	6.59	105.45	15.73	20.57	5.13
	TCT	30.95	4.94	109.77	12.28	28.75	3.82
	BL	30.95	4.94	109.77	12.28	28.75	3.82
	HC	30.95	4.94	109.77	12.28	28.75	3.82
simulation 3	SP	17.68	6.53	85.60	31.60	16.47	5.20
	TCT	26.53	4.90	94.41	24.56	24.67	3.83
	BL	26.53	4.90	94.41	24.56	24.67	3.83
	HC	26.53	4.90	94.41	24.56	24.67	3.83
simulation 6	SP	26.53	6.09	114.71	8.33	24.63	4.66
	TCT	30.95	4.98	120.26	3.90	30.52	3.94
	BL	30.95	4.98	117.29	6.27	29.81	3.93
	HC	30.95	4.98	118.34	5.43	29.91	3.96
simulation 7	SP	26.53	6.09	114.71	8.33	24.63	4.66
	TCT	26.53	4.97	107.99	13.70	26.28	4.11
	BL	26.53	4.97	106.71	14.73	26.06	4.10
	HC	26.53	4.97	104.03	16.87	25.60	4.06
simulation 8	SP	17.69	7.75	97.33	22.22	16.42	5.93
	TCT	22.10	4.95	92.75	25.88	21.92	4.23
	BL	22.10	4.95	91.07	27.23	21.74	4.19
	HC	22.10	4.95	91.71	26.71	21.74	4.22
simulation 9	SP	17.69	7.19	90.38	27.78	16.42	5.50
	TCT	17.68	4.93	75.98	39.28	17.55	4.33
	BL	17.68	4.93	73.00	41.67	17.19	4.25
	HC	17.68	4.93	73.70	41.11	17.18	4.29
simulation 10	SP	17.69	6.09	76.47	38.89	16.42	4.46
	TCT	17.68	4.91	73.75	41.07	17.41	4.24
	BL	17.68	4.91	72.67	41.93	17.23	4.22
	HC	17.68	4.91	72.34	42.19	17.23	4.20
simulation 18	SP	26.53	5.53	104.28	16.67	24.63	4.23
	TCT	17.68	4.96	77.22	38.29	17.55	4.40
	BL	17.68	4.96	77.22	38.29	17.55	4.40
	HC	17.68	4.96	77.22	38.29	17.55	4.40
simulation 19	SP	17.69	7.75	97.33	22.22	16.42	5.93
	TCT	17.68	4.94	74.96	40.10	17.42	4.30
	BL	17.68	4.94	74.96	40.10	17.42	4.30
	HC	17.68	4.94	74.96	40.10	17.42	4.30
simulation 20	SP	17.69	6.64	83.42	33.34	16.42	5.08
	TCT	17.68	4.92	72.98	41.68	17.29	4.22
	BL	17.68	4.92	72.98	41.68	17.29	4.22
	HC	17.68	4.92	72.98	41.68	17.29	4.22
simulation 21	SP	17.69	5.53	69.52	44.45	16.42	4.23
	TCT	17.68	4.90	71.17	43.13	17.16	4.15
	BL	17.68	4.90	71.17	43.13	17.16	4.15
	HC	17.68	4.90	71.17	43.13	17.16	4.15

to the maximum power of the respective panels with no shading, i.e. $P_m = 125.14\,W$.

It is observed that for simulation 1, all four configurations provide the same maximum power of $125.14W$, although at different maximum-power points. The SP configuration features a lower current and a higher voltage at the maximum-power point. For simulations 2 and 3, the complex configurations provide better maximum power than the SP configuration. That occurs in all those simulations in which the best result for the proposed reconfiguration of the SP panel (i.e. least power loss) is deemed to be that of the standard reference SP pattern, as shown in table II.

The SP configuration for simulations 6 & 7 provides equal power, since in both simulations the same connection pattern is suggested by the algorithm (see table II). However, the power production of the complex configurations is higher for simulation 6, but lower for simulation 7. This is due to the the fact that in simulation 6 only one cell is shaded, but two more fully illuminated cells are disconnected to achieve the suggested SP configuration, whereas in simulation 7 three cells are shaded. Therefore, the complex configurations are able to provide more power in simulation 6. As mentioned in section II., the TCT configuration performs best in comparison with the BL and HC configurations, because of its higher amount of ties. This can as well be observed in table II, in which, out of the three, the TCT configuration always shows the most promising results. In simulations 6 the TCT configuration only presents a power loss of 3.90%, whereas in simulation 7 its power loss is 13.70%. In comparison, the SP configuration presents for both simulations a relative power loss of 8.33%, thus outperforming the complex configurations in simulation 7.

Simulations 8 - 10 as well show a superior performance of the SP configuration, when reconnected properly. The differences between the SP and TCT configurations vary in magnitude for all three simulations. The results of simulation 8 & 10 are comparable in terms of the relative power reduction between the TCT and SP configuration. The difference in simulation 8 is 3.66%, due to the fact that additionally two fully illuminated PV cells had to be disconnected in the SP configuration. In simulation 10, on the other hand, it is only 2.16%, but here caused by the high number of shaded cells in general and the thereof resulting sparsity of fully illuminated cells to produce the necessary power. However, in simulation 9, where no additional fully illuminated cells had to be disconnected, the power loss reduction of the SP configuration in comparison to the TCT configuration is already up to 11.5%. Showing the strength of the reconfigurable SP pattern.

In simulations 18 - 20 the relative power loss reduction between the TCT and SP configuration can be seen to various degrees. Whereas in simulation 18 the reduction is more than half, from 38.29% to 16.67%, i.e. a difference of 21.62%, in simulations 19 & 20 it is less prominent, with a difference of only 17.88% and 8.34%, respectively. Generally speaking, it can be observed that the relative power loss reduction decreases with an increase in shaded cells. This observation can, as well, be extended to simulation 21. Here the TCT configuration outperforms the SP configuration by 1.32%. In it, 16 PV cells are shaded and the SP configuration cannot count on enough fully illuminated cells anymore.

The results suggest that for shading patterns with more than 14 photovoltaic cells the complex fixed configurations (TCT, BL and HC) perform better than the SP configuration. This can be seen considering simulation 10 and 21. In the first, the SP configuration could still outperform the TCT configuration slightly, with 14 shaded PV cells. In the second, this was not possible anymore with 16 shaded PV cells.

The herein proposed SP reconfigurable panel or any of the three analyzed fixed complex configurations, of which the TCT is the best, may offer a reduction to the power loss when shading is present. In some shading conditions, the reconfigurable panel outperforms the complex configurations. However, its practical implementation requires a rather intricate interconnect and signal-bus grid, a number of switches per cell, sensing capability at each cell and a microcontroller unit. These additional components also require power and might, therefore, consume the additional power saved by the proposed configuration, which must be carefully considered. The TCT fixed connection, on the other hand, only requires some additional interconnects compared to conventional panel. Nevertheless, the reconfigurable panel might still be a more appealing choice in micro-energy harvesting for autonomous integrated electronic systems, or systems on chip for the Internet of Things (IoT). In such cases any energy saving is important, interconnection complexity is not an issue, switches and sensors can be easily and distributedly integrated and a processor can be native to the system. Besides, the cells, equipped with switches, could also more easily double as optical detectors, for example in LiFi (Light-Fidelity) optical communication systems.

VII. Conclusion

When PV panels are shaded to any extent, their power output is reduced. The aim of this work was to conceive and simulate a smart reconnection strategy for PV panels that is able to mitigate the current shading situation.

The reconfigurable panel adopting the proposed strategy should be able to reconnect and disconnect its PV cells to adapt to the situation at hand and provide the maximum possible power output. This strategy could also be applied to other detrimental cell conditions that lead to an ill-performing panel, either due to the cells or to the encapsulation, as local hot spots, inhomogeneous ageing and degradation, electrical breakdown, optical opacity or mechanical damage. The panel internally implementing this strategy can also work together with an external Maximum-Power-Point Tracker (MPPT) algorithm.

Therefore, an algorithm was developed to simulate separate PV cells and associate them in a panel. It assesses the I-V characteristics of each cell and that of each possible series-parallel connection pattern for the number of cells available in the panel, under the current environmental and shading conditions. It then determines the best configuration, considering pre-defined voltage and power boundaries.

A 36-cell photovoltaic panel, based on the Kyocera KD140SX-UFBS, was simulated for an irradiance of $500\ W/m^2$. Different and progressive shading patterns have been applied and their effects have been analyzed. It was

found that, for diagonal and horizontal shading patterns the power loss can be reduced in comparison to the chosen standard series-parallel (SP) configuration ($N_s = 12$ and $N_p = 3$) and complex configurations (Total Cross-Tied, TCT; Bridge Linked, BL; and Honey Comb, HC). In relation to the shaded standard configuration, at least $5\ W$, or 4%, can be gained. For some shading patterns, even 32% of the overall power under ideal conditions, which corresponds to about 39W, can be recovered. When compared to the complex configurations, the power loss can be reduced by 2% to 22%. However, these results were only achievable for shading patterns where a maximum of 14 solar cells had been in the dark. When more than 14 PV cells are affected and in vertical shading, the algorithm was not able to determine suitable configurations to reduce the power loss.

Even though it is possible that fixed complex configurations offer comparable power loss reductions to the herein presented reconfigurable panel, the latter might still be appealing for micro-energy harvesting in autonomous integrated devices. For which any energy saving is a key issue. Conveniently, the introduction of switches and the implementation of a dynamic algorithm in hardware is compatible with integrated-system technologies. Besides energy harvesting, making use of the integrated switches, the cells could also double as receivers in free-space optical communication systems.

ACKNOWLEDGEMENTS

The authors are thankful to engineers Diogo Ferraz Costa and Poliana Bueno for their input on some of the PV simulations. They also thank PPGEE (Graduate Program on Electrical Engineering - UFMG), FAPEMIG (Research Foundation of the State of Minas Gerais - Brazil) and CNPq (National Research Council - Brazil) for institutional support and financial resources. This study was financed in part by the Coordenação de Aperfeiçoamento de Pessoal de Nível Superior - Brasil (CAPES) - Finance Code 001.

REFERENCES

[1] J. H. de Oliveira, "Impactos de flutuaçoes de potência e compensaçao de reativos na rede elétrica: Estudo de caso da usina fotovoltaica do mineirao." Master's thesis, Universidade Federal de Minas Gerais, 2016.

[2] R. P. Gruber, "Self-reconfiguring solar cell system," Alexandria, VA, USA, Nov. 1979, uS Patent 4,175,249. [Online]. Available: https://www.google.com.br/patents/US4175249

[3] Z. M. Salameh and F. Dagher, "The effect of electrical array reconfiguration on the performance of a PV-powered volumetric water pump," *IEEE Transactions on Energy Conversion*, vol. 5, no. 4, pp. 653–658, Dec. 1990. [Online]. Available: http://dx.doi.org/10.1109/60.63135

[4] Y. Auttawaitkul, B. Pungsiri, K. Chammongthai, and M. Okuda, "A method of appropriate electrical array reconfiguration management for photovoltaic powered car," in *IEEE Asia-Pacific Conference on Circuits and Systems. Microelectronics and Integrating Systems. Proceedings (Cat. No.98EX242)*. IEEE, 1998, pp. 201–204. [Online]. Available: http://dx.doi.org/10.1109/APCCAS.1998.743713

[5] C. L. Craig, "Solar array switching unit," Alexandria, VA, USA, May 2000, uS Patent 6,060,790. [Online]. Available: https://www.google.com/patents/US6060790

[6] R. A. Sherif and K. S. Boutros, "Solar module array with reconfigurable tile," Alexandria, VA, USA, Feb. 2002, uS Patent 6,350,944. [Online]. Available: https://www.google.com/patents/US6350944

[7] D. Nguyen and B. Lehman, "An adaptive solar photovoltaic array using Model-Based reconfiguration algorithm," *IEEE Transactions on Industrial Electronics*, vol. 55, no. 7, pp. 2644–2654, Jul. 2008. [Online]. Available: http://dx.doi.org/10.1109/TIE.2008.924169

[8] G. Velasco-Quesada, F. Guinjoan-Gispert, R. Pique-Lopez, M. Roman-Lumbreras, and A. Conesa-Roca, "Electrical PV array reconfiguration strategy for energy extraction improvement in Grid-Connected PV systems," *IEEE Transactions on Industrial Electronics*, vol. 56, no. 11, pp. 4319–4331, 2009. [Online]. Available: http://dx.doi.org/10.1109/TIE.2009.2024664

[9] B. Patnaik, P. Sharma, E. Trimurthulu, S. P. Duttagupta, and V. Agarwal, "Reconfiguration strategy for optimization of solar photovoltaic array under non-uniform illumination conditions," in *37th IEEE Photovoltaic Specialists Conference*. Seattle, WA, USA: IEEE, Jun. 2011, pp. 001 859–001 864. [Online]. Available: http://dx.doi.org/10.1109/PVSC.2011.6186314

[10] M. Z. S. El-Dein, M. Kazerani, and M. M. A. Salama, "Optimal photovoltaic array reconfiguration to reduce partial shading losses," *IEEE Transactions on Sustainable Energy*, vol. 4, no. 1, pp. 145–153, 2013. [Online]. Available: http://dx.doi.org/10.1109/TSTE.2012.2208128

[11] M.-I. Baka, F. Catthoor, and D. Soudris, "Near-static shading exploration for smart photovoltaic module topologies based on snake-like configurations," *ACM Transactions on Embedded Computing Systems (TECS)*, vol. 15, no. 2, p. 27, 2016.

[12] P. Bauwens, J. Govaerts, M. Baka, F. Catthoor, K. Baert, G. Van den Broeck, H. Goverde, D. Anagnostos, J. Doutreloigne, and J. Poortmans, "Reconfigurable topologies for smarter pv modules: simulation, evaluation and implementation," in *32nd EU PVSEC*, 2016, pp. 61–65.

[13] A. Eick, "Reconnection Patterns of Photovoltaic Cells to Reduce Power Loss Due to Detrimental Conditions," Master's thesis, Universidade Federal de Minas Gerais, 2017. [Online]. Available: https://www.ppgee.ufmg.br/diss_defesas_detalhes.php?aluno=1420

[14] A. Laudani, G. M. Lozito, V. Lucaferri, M. Radicioni, and F. R. Fulginei, "On circuital topologies and reconfiguration strategies for pv systems inpartial shading conditions: A review," *AIMS Energy*, vol. 6, no. 5, pp. 735–763, 2018.

[15] S. Daliento, F. Di Napoli, P. Guerriero, and V. d'Alessandro, "A modified bypass circuit for improved hot spot reliability of solar panels subject to partial shading," *Solar Energy*, vol. 134, pp. 211–218, 2016.

[16] S. R. Pendem and S. Mikkili, "Modeling, simulation, and performance analysis of pv array configurations (series, series-parallel, bridge-linked, and honey-comb) to harvest maximum power under various partial shading conditions," *International Journal of Green Energy*, vol. 15, pp. 1–18, 10 2018.

[17] B. Celik, E. Karatepe, S. Silvestre, N. Gökmen, and C. Aissa, "Analysis of spatial fixed pv arrays configurations to maximize energy harvesting in bipv applications," *Renewable Energy*, vol. 75, pp. 534–540, 11 2014.

[18] N. D. Kaushika and N. K. Gautam, "Energy yield simulations of interconnected solar PV arrays," *IEEE Transactions on Energy Conversion*, vol. 18, no. 1, pp. 127–134, Mar. 2003. [Online]. Available: http://dx.doi.org/10.1109/TEC.2002.805204

[19] Y.-J. Wang and P.-C. Hsu, "Analysis of partially shaded PV modules using piecewise linear parallel branches model," *International Journal of Electrical, Computer, Energetic, Electronic and Communication Engineering*, vol. 3, no. 12, pp. 2354–2360, 2009. [Online]. Available: http://waset.org/Publications?p=36

[20] R. Ramaprabha and B. L. Mathur, "A comprehensive review and analysis of solar photovoltaic array configurations under partial shaded conditions," *International Journal of Photoenergy*, vol. 2012, 2012.

[21] J. J. Soon, K.-S. Low, and S. T. Goh, "Multi-dimension diode photovoltaic (pv) model for different pv cell technologies," *IEEE 23rd International Symposium on Industrial Electronics (ISIE)*, pp. 2496–2501, Jun 2014.

[22] L. Castañer and S. Silvestre, *Modelling PV Systems Using PSpice*. West Sussex, England: John Wiley and Sons, 2002.

[23] A. Eick, "Electrical Characterization of Photovoltaic Cells to Predict Cell Performance," 2015. [Online]. Available: https://www.hbo-kennisbank.nl/record/oai:repository.samenmaken.nl:smpid:57050

[24] G. H. Hardy and E. M. Wright, *An introduction to the theory of numbers*, 4th ed. Oxford, Great Britain: Oxford University Press, 1975.

[25] S. Suckow, "2/3-Diode fit," Aachen, Germany, 2014. [Online]. Available: https://nanohub.org/resources/14300